Ecological and evolutionary implications of starvation and body size

Justin D. Yeakel * † ‡, **Christopher P. Kempes** †, **and Sidney Redner** † §

*School of Natural Science, University of California Merced, Merced, CA,†The Santa Fe Institute, Santa Fe, NM,§Department of Physics, Boston University, Boston MA, and ‡To whom correspondence should be addressed: jdyeakel@gmail.com

Submitted to Proceedings of the National Academy of Sciences of the United States of America

This is the abstract.

The behavioral ecology of most, if not all, organisms is influenced by the energetic state of individuals, which directly influences how organisms invest reserves in uncertain environments. Such behaviors are generally manifested as trade-offs between investing in somatic maintenance and growth or allocating energy towards reproduction [1, 2, 3]. The timing of these behaviors is often important and is under strong selective pressure, as it tends to directly impact future fitness [4]. Importantly, the influence of resource limitation on an organism's ability to maintain its nutritional stores may lead to repeated delays or shifts in reproduction over the course of an organism's life.

Maximizing fitness between growth and maintenance activities vs. reproduction structures the life-history of many species, and this can be achieved by alternative behavioral strategies conditioned on resource availability [5]. For example, reindeer invest less in calves born after harsh winters (when the mother's energetic state is poor) than in calves born after moderate winters [6], ~~whereas~~ many bird species invest differently in broods during periods of resource scarcity [7, 8], sometimes delaying or foregoing reproduction for a breeding season [1, 9, 10]. ~~Even~~ freshwater and marine zooplankton have been observed to avoid reproduction under nutritional stress [11], with those that do reproduce have lower survival rates [2]. Organisms may also separate maintenance and growth from reproduction over space and time: many salmonids, birds, and some mammals return to migratory breeding grounds to reproduce after one or multiple seasons ~~in alternative environments spent~~ accumulating nutritional reserves [12, 13, 14].

Physiological mechanisms also play an important role in regulating reproductive expenditures during periods of resource limitation. Diverse mammals (47 species in 10 families) exhibit delayed implantation whereby females postpone fetal development (blastocyst implantation) to time with accumulation of nutritional reserves [15, 16], while many others (including humans) suffer irregular menstrual cycling and higher abortion rates during periods of nutritional stress [17, 18]. In the extreme case of unicellular organisms, nutrition is unavoidably linked to reproduction because the nutritional state of the cell regulates all aspects of the cell cycle [19]. The existence of so many independently evolved mechanisms across such a diverse suite of organisms points to the importance and universality of the fundamental tradeoff between somatic and reproductive investment, however the dynamic implications of these constraints are unknown.

Though straightforward conceptually, incorporating the energetic dynamics of individuals [20] into a population-level framework [20, 21] presents numerous mathematical obstacles (in particular a lack of smoothness or differentiability [22]), and is prone to over-fitting. An alternative approach involves modeling the macroscale relationships that guide somatic vs. reproductive investment in a consumer-resource system. Macroscale Lotka-Volterra models assume a dependence of consumer population growth rates on resource density, thus *implicitly* incorporating the requirement of resource availability for reproduction [23]. Resource limitation and the subsequent effects of starvation may be alternatively accounted for *explicitly*, such that reproduction is permitted only for individuals with sufficient energetic reserves. Such a dynamic introduces i) the reproductive time lag associated with changing rates of starvation and recovery, and ii) the idea that reproduction is strongly allometrically constrained [3], and not generally linearly related to resource density.

Nutritional state-structured model (NSM)

We explore how the energetic tradeoff between somatic maintenance and growth vs. reproduction can influence population dynamics, and how such dynamics may be constrained by allometry. We begin by establishing a minimal Nutritional State-structured population Model (NSM), where the consumer population is divided into two energetic states: i) an energetically replete (full) state F, where the consumer reproduces at a constant rate λ, and ii) an energetically deficient (hungry) state H, where reproduction is suppressed, and mortality occurs at rate μ. The resource R has logistic growth with an intrinsic growth rate α and carrying capacity of unity. Consumers transition from state F to state H by starvation at rate σ and in proportion to the lack of resources $(1-R)$. Conversely, consumers recover from state H to the full state F at rate ρ and in proportion to R. Resources are eliminated by the consumer in both states: by energetically deficient consumers at rate ρ, and by energetically replete consumers at rate β. Accordingly, the system of equations is written

$$\begin{aligned}
\dot{F} &= \lambda F + \rho R H - \sigma(1-R)F, \\
\dot{H} &= \sigma(1-R)F - \rho R H - \mu H, \\
\dot{R} &= \alpha R(1-R) - R(\rho H + \beta F).
\end{aligned} \qquad [\mathbf{0}]$$

There are three fixed points associated with the NSM: two trivial fixed points at $(R^* = 0, H^* = 0, F^* = 0)$ and $(R^* = 1, H^* = 0, F^* = 0)$, and one internal fixed point at

Reserved for Publication Footnotes

$$
\begin{aligned}
F^* &= \frac{\alpha\lambda\mu(\mu+\rho)}{(\lambda\rho+\mu\sigma)(\lambda\rho+\mu\beta)}, \\
H^* &= \frac{\alpha\lambda^2(\mu+\rho)}{(\lambda\rho+\mu\sigma)(\lambda\rho+\mu\beta)}, \\
R^* &= \frac{\mu(\sigma-\lambda)}{\lambda\rho+\mu\sigma}.
\end{aligned}
\qquad [\mathbf{0}]
$$

Because there is only one internal fixed point, as long as it is stable the population trajectories will serve as a global attractor for any set of initial conditions > 0. Stability is determined with respect to the Jacobian Matrix $\mathbf{J}|_*$ (where $|_*$ denotes evaluation at the internal steady state), where each element of the matrix is defined by the partial derivative of each differential equation with respect to each variable. If the parameters of $\mathbf{J}|_*$ are such that the real part of its leading eigenvalue is < 0, then the system is stable to small pulse perturbations.

Allometric rates

The parameters in the NSM cannot be freely navigated in biologically-reasonable settings, and our first challenge is to constrain the covariation of rates in a principled and biologically meaningful manner. Allometric scaling relationships highlight common constraints and average trends across large ranges in body size and species diversity. Many of these relationships can be derived from a small set of assumptions and below we describe a framework for the covariation of timescales and rates across the range of mammals for each of the key parameters of our model (cf. [24]). We are able to define the regime of dynamics occupied by the entire class of mammals along with the key differences between the largest and smallest mammals.

Nearly all of the rates described in the NSM are to some extent governed by consumer metabolism, and thus can be estimated based on known allometric constraints. The scaling relationship between an organism's metabolic rate B and its body size at reproductive maturity M is well documented [25] and plays a central role in a variety of scaling relationships. Organismal metabolic rate B is known to scale as $B = B_0 M^{\eta}$, where η is the scaling exponent, generally assumed to be 3/4 for metazoans, and varies in unicellular species between $\eta \approx 1$ in eukaryotes and $\eta \approx 1.76$ in bacteria [26]. Several efforts have shown how a partitioning of this metabolic rate between growth and maintenance purposes can be used to derive a general equation for the growth trajectories and growth rates of organisms ranging from bacteria to metazoans [3]. More specifically, the interspecific trends in growth rate can be approximated by $\lambda = \lambda_0 M^{\eta-1}$. This relationship is derived from the simple balance

$$
B_0 m^{\eta} = E_m \frac{dm}{dt} + B_m m \qquad [\mathbf{0}]
$$

[a and b notation — these parameters are easily measured bioenergetic parameters which are often approximately invariant across organisms of vastly different size. Our notation seeks to illustrate that the allometric model fundamentally depends on a small number of free parameters.] where E_m is the energy needed to synthesize a unit of mass, B_m is the metabolic rate to support an existing unit of mass, and m is the mass at any point in development. It is useful to explicitly write this balance because it can also be modified to understand the rates of both starvation and recovery from starvation. [Spell out the connection to nutritional state more explicitly] [As we will see it is possible to derive both sigma and rho from this balance]

For the rate of starvation, we make the simple assumption that an organism must meet its maintenance requirements using digested mass as the sole energy source. This assumption implies the simple metabolic balance

$$
\frac{dm}{dt} E'_m = -B_m m \qquad [\mathbf{0}]
$$

where E'_m is the amount of energy stored in a unit of existing body mass which may differ from E_m, the energy required to synthesis a unit of biomass. Give the adult mass, M, of an organism this energy balance prescribes the mass trajectory of a starving organism:

$$
m(t) = M e^{-B_m t / E'_m}. \qquad [\mathbf{0}]
$$

Considering that only certain tissues can be digested for energy, for example the brain cannot be degraded to fuel metabolism, we define the rate for starvation and death by the timescales required to reach specific fractions of normal adult mass. We define $m_{starve} = \epsilon M$ where it could be the case that organisms have a systematic size-dependent requirement for essential tissues, such as the minimal bone or brain mass. For example, considering the observation that body fat in mammals scales with overall body size according to $M_f = f_0 M^{\gamma}$, and assuming that once this mass is fully digested the organism begins to starve, would imply that $\epsilon = 1 - f_0 M^{\gamma}/M$. Taken together the time scale for starvation is given by

$$
t_{\sigma} = -\frac{E_m \log(\epsilon)}{B_m}. \qquad [\mathbf{0}]
$$

The starvation rate is $\sigma = 1/t_{\sigma}$, which implies that σ is independent of adult mass if ϵ is a constant, and if ϵ does scale with mass, then σ will have a factor of $1/\log(1 - f_0 M^{\gamma}/M)$. In either case σ does not have a simple scaling with λ which is important for the dynamics that we later discuss.

The time to death should follow a similar relationship, but defined by a lower fraction of adult mass, $m_{death} = \epsilon' M$. Consider, for example, that an organism dies once it has digested all fat and muscle tissues, and that muscle tissue scales with body mass according to $M_{mm} = mm_0 M^{\zeta}$, then $\epsilon' = 1 - \left(f_0 M^{\gamma} + mm_0 M^{\zeta}\right)/M$. Muscle mass has been shown to be roughly proportional to body mass [**?**] in mammals and thus ϵ' is effectively ϵ minus a constant. Thus

$$
t_{\mu} = -\frac{E_m \log(\epsilon')}{B_m} \qquad [\mathbf{0}]
$$

and $\mu = 1/t_{\mu}$.

The rate of recovery $\rho = 1/t_{\rho}$ requires that an organism accrues tissue from the starving state to the full state. We again use the balance given in Equation to find the timescale to return to the mature mass from a given reduced starvation mass. The general solution to Equation is given by

$$
m(t) = c\left[1 - \left(1 - \frac{b}{a} m_0^{1-\eta}\right) e^{-b(1-\eta)t}\right]^{1/(1-\eta)} \qquad [\mathbf{0}]
$$

with $a = B_0/E_m$, $b = B_m/E_m$, and $c = (a/b)^{1/(\eta-1)}$. We are then interested in the timescale, $t_{\rho} = t_2 - t_1$, which is the time it takes to go from $m(t_1) = \epsilon M$ to $m(t_2) = M$, which has the final form of

$$
t_{\rho} = \frac{\log\left(1 - (cM)^{1-\eta}\right) - \log\left(1 - (c\epsilon M)^{1-\eta}\right)}{(\eta - 1)b}. \qquad [\mathbf{0}]
$$

Although these rate equations are general, here we focus on parameterizations for terrestrial-bound endotherms, specifically mammals, which range from $M \approx 1$ gram (the Etruscan shrew *Suncus etruscus*) to $M \approx 10^7$ grams (the late Eocene to early Miocene Indricotheriinae). Investigating other classes of organisms requires only substituting the energetic and scale parameters shown in Table 1. Moreover, we emphasize that our allometric equations describe mean relationships, and do not account for the (sometimes considerable) variance associated with individual species.

The stabilizing effects of allometric constraints

Stability in the NSM is conditioned on the consumer's starvation rate σ relative to its reproduction rate λ. If $\sigma < \lambda$, the resource steady state density is negative and extinction is inevitable. The condition $\sigma = \lambda$ is a transcritical (TC) bifurcation, thus marking a hard boundary below which the system is unphysical due to the unregulated growth of the consumer population. That the timescale of reproduction is larger than the timescale of starvation is intuitive for macroscopic organisms, as the rate at which one loses tissue due to a lack of resources is generally much faster than reproduction. In fact, allometric derivations for both reproduction [3] and starvation (Eq.) show that this relationship always holds for organisms within observed body size ranges (Fig. 2).

In addition to the hard bound defined by the TC bifurcation, oscillating or cyclic dynamics present an implicit constraint to persistence by increasing extinction risk due to stochastic effects. In continuous-time systems, a stable limit cycle arises when a pair of complex conjugate eigenvalues crosses the imaginary axis to attain positive real parts [27]. This condition, known as a Hopf bifurcation, is defined by $\mathrm{Det}(\mathbf{S}) = 0$, where $\mathbf{S}$ is the Sylvester matrix, which is composed of the coefficients of the characteristic polynomial describing the Jacobian [28]. Moreover, as a non-cyclic stable system nears the Hopf bifurcation, transient or decaying cycles can grow in magnitude, despite the existence of a positive, non-cyclic, steady state density. Given that ecological systems exist in a state of constant perturbation [29], even the onset of transient cycles that decay over time can increase the risk of extinction [30, 31, 32], such that the distance of a system from the Hopf bifurcation is relevant to persistence.

The NSM exhibits both non-cyclic as well as cyclic dynamics, and which behavior dominates depends strongly on the rate of starvation σ relative to the rate of recovery ρ. Although starvation leads to mortality risk, a moderate amount promotes persistence of both consumer and resource populations as non-cyclic stability of the fixed point generally requires a higher σ relative to ρ. The intuition behind this is that transition to the hungry (non-reproductive) state permits the resource to recover and transient dynamics to subside, whereas a low σ overloads the system with energetically-replete (reproducing) individuals, maintaining oscillations between consumer and resource (Fig. 3). If σ is too large, mortality due to starvation depletes the consumer population, resulting in a lower steady state density for the consumer and a higher steady state density for the resource.

Whereas the rate of consumer growth defines a hard bound of biological feasibility (the TC bifurcation), the rate of starvation thus determines the sensitivity of the consumer population to changes in resource density. While higher rates of starvation result in lower steady state population size – increasing the risk of stochastic extinction – lower rates of starvation result in a system poised near either the TC or Hopf bifurcation, which will lead to elimination of the resource or the development of cyclic oscillations, respectively. Which bifurcation is approached is wholly dependent on the rate of recovery: if it is high, then cyclic dynamics will develop; if it is low, resource extinction becomes increasingly likely.

As the allometric derivations of NSM rate laws reveal, σ and ρ are not independent parameters, and the bifurcation space shown in Fig. 3 cannot be freely navigated if assuming biologically reasonable parameterizations. Given the parameterization for terrestrial endotherms shown in Table 1 with mass M as a free parameter, we show that σ and ρ are constrained to a small window of potential values (Fig. 4), thus confining dynamics to the steady state regime for all realized body size classes. Moreover, for larger M, the distance to the Hopf bifurcation increases, while uncertainty in allometric parameters (20% variation around the mean; Fig. 4) results in little qualitative difference. This suggests that small mammals are more prone to population oscillations – including both stable limit cycles as well as transient cycles – than mammals with larger body size.

Allometric constraints have been invoked to explain the periodicity of cyclic populations [33, 34, 35], such that period $\propto M^{0.25}$, however this relationship seems to hold only for some species [36] and competing explanations exist [37, 38]. Statistically significant support for the existence of population cycles among mammals is predominantly based on time-series for smaller bodied mammals [39], though we acknowledge that longer generation times precludes similar quality data for larger organisms. We thus obtain a specific prediction from our model: population cycles should be less common for larger species and more common for smaller species, particularly in environments where resources are limiting.

Higher rates of starvation result in a larger flux of the population to the hungry state, eliminating reproduction and increasing the likelihood of mortality, however it is the rate of starvation relative to the rate of recovery that determines the long-term dynamics of the system (Fig 3). We examine the competing effects of cyclic dynamics vs. changes in steady state density on extinction risk as a function of the ratio σ/ρ. We computed the probability of extinction, where extinction is defined as $H(t) + F(t) = 10$ at any instant across all values of $10^2 < t \leq 10^6$, for 1000 replicates of the continuous-time system shown in Eq. for an organism of $M = 100$ grams, assuming random initial conditions around the steady state (Eq.). By allowing the rate of starvation to vary, we assessed extinction risk across a range of values of the ratio σ/ρ varying between 10^{-2} to 2.5, thus examining a horizontal cross-section of Fig. 3. As expected, higher rates of extinction correlated with both low and high values of σ/ρ; for low values the higher extinction risk results from transient cycles with larger amplitudes as the system nears the Hopf bifurcation (Fig. 5). For large values of σ/ρ, higher extinction risk is due to the decrease in the steady state consumer population density. This interplay creates an 'extinction refuge' as shown in Fig. 5, such that for a relatively constrained range of σ/ρ, extinction probabilities are minimized.

As has been described, the σ vs. ρ space cannot be freely traversed, such that not all values of σ/ρ are biologically feasible. We observe that the allometrically constrained values of σ/ρ (with $\pm 20\%$ variability around energetic parameter means) fall within the extinction refuge, such that they are close enough to the Hopf bifurcation to avoid low steady state densities, though far enough away to avoid large-amplitude transient cycles. The fact that allometric values of σ and ρ fall within this relatively small window supports the possibility that a selective mechanism has constrained the physiological conditions driving observed starvation and recovery rates within populations. Such a mechanism would involve a feedback between the dynamics of the population and the fitness of individuals within the population, though to what extent the dynamics of the population influence rates of starvation and recovery would also involve potential tradeoffs in reproduction and somatic maintenance. Nevertheless, our finding that allometrically-determined energetic rates place the system within this low extinction probability region suggests that the NSM system provides general insight to a phenomena that may both drive – and constrain – natural animal populations.

Dynamic and energetic barriers to body size

Metabolite transportation constraints are widely thought to place strict boundaries on biological scaling [40, 41, 42], leading to specific predictions on the minimum possible body size for organisms [43]. Above this bound, a number of energetic and evolutionary mechanisms have been explored to assess the costs and benefits associated with larger body masses, particularly for mammals. The *fasting endurance hypothesis* contends that larger body size, with lower metabolic rates and able to hold more endogenous energetic reserves, may buffer organisms against environmental fluctuations in resource availability [44]. Over evolutionary time, terrestrial mammalian lineages show a significant trend towards larger body size (known as Cope's Rule) [45, 46, 47, 48], and it is thought that within-lineage drivers generate selection towards an optimal upper-bound of ca. 10^7 grams [45], the value of which may arise from higher extinction risk for large taxa over evolutionary timescales [46]. These trends are thought to be driven by a combination of climate change and niche availability [48], however the underpinning energetic costs and benefits of larger body sizes, and how they influence dynamics over ecological timescales, has not been explored, and we contend that the NSM provides a suitable framework to explore these issues.

The NSM correctly predicts that species with smaller masses have larger steady state population densities, however we observe that there is a sharp asymptote in both steady state densities as well as σ/ρ at $M \approx 0.3$ grams (Fig. 6a,b). Observation of the rates of starvation and recovery explain why: as mass decreases, the rate of starvation increases, while the rate of recovery declines super-exponentially. This decline in ρ occurs when body fat percentage is $1-1/(cM) \approx 2\%$, whereupon consumers have no eligible route out of starvation. Compellingly, this dynamic bound determined by the rate of energetic recovery is close to the minimum observed mammalian body size of ca. 1.3-2.5 grams (Fig. 6b,c), a range that occurs as the recovery rate begins its decline. In addition to known transport limitations [43], we suggest that an additional constraint of lower body size stems from the dynamics of starvation.

Although there are upper bounds to the rate equations (e.g. when percent body fat becomes unity), they are not biologically feasible and we do not discuss them further. Instead, we examine a potential upper bound to body mass by assessing population invasibility with respect to a mutated subset of the population (denoted by $'$) where individuals have a modified proportion of body fat $M' = M(1+\chi)$ where $\chi \in [-0.5, 0.5]$, thus altering rates of starvation, recovery, and maintenance β. Although there is not an internal fixed point where both residents and invaders coexist (except for the trivial state $\chi = 0$), we can assess invasibility as a function of organismal mass by determining which consumer steady state is larger over χ. We find that for $1 \leq M < 10^6$g, having additional body fat ($\chi > 0$) results in a higher steady state density for the invader population ($H'^* + F'^* > H^* + F^*$), such that it has an intrinsic advantage over the resident population. For $M > 10^6$, however, there is an increasing range of $\chi < 0$ such that leaner individuals have the advantage, and this is due to the changing covariance between energetic rates as a function of modified energetic reserves.

The observed switch in invasibility as a function of χ at $M_{\mathrm{opt}} \approx 10^6$ thus serves as an attractor, where over evolutionary time the NSM predicts organismal mass to increase if $M < M_{\mathrm{opt}}$ and decrease if $M > M_{\mathrm{opt}}$. Moreover, M_{opt}, which is entirely determined by the population-level consequences of energetic constraints is within an order of magnitude as that observed in the North American mammalian fossil record [45] and as that predicted from an evolutionary model of body size evolution [46]. While the state of the environment, as well as the competitive landscape, will determine whether specific body size sizes are selected for or against [48], we suggest that the starvation dynamic proposed here may supply the fundamental momentum fueling the evolution of larger body size among terrestrial mammals.

The energetics associated with somatic maintenance, growth, and reproduction are important elements that influence the dynamics of all populations [9]. The NSM is a minimal and general model that incorporates the dynamics of starvation that are expected to occur in resource limited environments. By incorporating allometric relationships between the rates in the NSM, we find *i*) different organismal masses are more or less prone to different population dynamic regimes, *ii*) allometrically-determined rates of starvation and recovery appear to minimize extinction risk, and *iii*) the dynamic consequences of these rates may place additional barriers on the evolution of minimum and maximum body size. We suggest that the NSM offers a means by which the dynamic consequences of energetic constraints can be assessed using macroscale interactions between and among species. Future efforts will involve exploring the consequences of these dynamics in a spatially explicit framework, thus incorporating elements such as movement costs and spatial heterogeneity, which may elucidate additional tradeoffs associated with the dynamics of starvation.

1. Martin TE (1987) Food as a Limit on Breeding Birds: A Life-History Perspective. *Annu. Rev. Ecol. Syst.* 18:453–487.
2. Kirk KL (1997) Life-History Responses to Variable Environments: Starvation and Reproduction in Planktonic Rotifers. *Ecology* 78:434–441.
3. Kempes CP, Dutkiewicz S, Follows MJ (2012) Growth, metabolic partitioning, and the size of microorganisms. *PNAS* 109:495–500.
4. Mangel M, Clark CW (1988) *Dynamic Modeling in Behavioral Ecology* (Princeton University Press, Princeton).
5. Morris DW (1987) Optimal Allocation of Parental Investment. *Oikos* 49:332.
6. Tveraa T, Fauchald P, Henaug C, Yoccoz NG (2003) An examination of a compensatory relationship between food limitation and predation in semi-domestic reindeer. *Oecologia* 137:370–376.
7. Daan S, Dijkstra C, Drent R, Meijer T (1988) *Food supply and the annual timing of avian reproduction.*
8. Jacot A, Valcu M, van Oers K, Kempenaers B (2009) Experimental nest site limitation affects reproductive strategies and parental investment in a hole-nesting passerine. *Animal Behaviour* 77:1075–1083.
9. Stearns SC (1989) Trade-Offs in Life-History Evolution. *Funct. Ecol.* 3:259.
10. Barboza P, Jorde D (2002) Intermittent fasting during winter and spring affects body composition and reproduction of a migratory duck. *J Comp Physiol B* 172:419–434.
11. Threlkeld ST (1976) Starvation and the size structure of zooplankton communities. *Freshwater Biol.* 6:489–496.
12. Weber TP, Ens BJ, Houston AI (1998) Optimal avian migration: A dynamic model of fuel stores and site use. *Evolutionary Ecology* 12:377–401.
13. Mduma SAR, Sinclair ARE, Hilborn R (1999) Food regulates the Serengeti wildebeest: a 40-year record. *J. Anim. Ecol.* 68:1101–1122.
14. Moore JW, Yeakel JD, Peard D, Lough J, Beere M (2014) Life-history diversity and its importance to population stability and persistence of a migratory fish: steelhead in two large North American watersheds. *J. Anim. Ecol.*
15. Mead RA (1989) in *Carnivore Behavior, Ecology, and Evolution* (Springer US, Boston, MA), pp 437–464.
16. Sandell M (1990) The Evolution of Seasonal Delayed Implantation. *The Quarterly Review of Biology* 65:23–42.
17. Bulik CM, et al. (1999) Fertility and Reproduction in Women With Anorexia Nervosa. *J. Clin. Psychiatry* 60:130–135.
18. Trites AW, Donnelly CP (2003) The decline of Steller sea lions Eumetopias jubatus in Alaska: a review of the nutritional stress hypothesis. *Mammal Review* 33:3–28.
19. Glazier DS (2009) Metabolic level and size scaling of rates of respiration and growth in unicellular organisms. *Funct. Ecol.* 23:963–968.
20. Kooijman SALM (2000) *Dynamic Energy and Mass Budgets in Biological Systems* (Cambridge).
21. Sousa T, Domingos T, Poggiale JC, Kooijman SALM (2010) Dynamic energy budget theory restores coherence in biology. *Philos. T. Roy. Soc. B* 365:3413–3428.
22. Diekmann O, Metz JAJ (2010) How to lift a model for individual behaviour to the population level? *Philos. T. Roy. Soc. B* 365:3523–3530.
23. Murdoch WW, Briggs CJ, Nisbet RM (2003) *Consumer-resource Dynamics*, Monographs in population biology (Princeton University Press).
24. Yodzis P, Innes S (1992) Body Size and Consumer-Resource Dynamics. *Am. Nat.* 139:1151–1175.

25. West GB, Woodruff WH, Brown JH (2002) Allometric scaling of metabolic rate from molecules and mitochondria to cells and mammals. *Proc. Natl. Acad. Sci. USA* 99 Suppl 1:2473–2478.

26. DeLong JP, Okie JG, Moses ME, Sibly RM, Brown JH (2010) Shifts in metabolic scaling, production, and efficiency across major evolutionary transitions of life. *PNAS* 107:12941–12945.

27. Guckenheimer J, Holmes P (1983) *Nonlinear oscillations, dynamical systems, and bifurcations of vector fields* (Springer, New York).

28. Gross T, Feudel U (2004) Analytical search for bifurcation surfaces in parameter space. *Physica D* 195:292–302.

29. Hastings A (2001) Transient dynamics and persistence of ecological systems. *Ecol. Lett.* 4:215–220.

30. Neubert M, Caswell H (1997) Alternatives to resilience for measuring the responses of ecological systems to perturbations. *Ecology* 78:653–665.

31. Caswell H, Neubert MG (2005) Reactivity and transient dynamics of discrete-time ecological systems. *Journal of Difference Equations and Applications* 11:295–310.

32. Neubert M, Caswell H (2009) Detecting reactivity. *Ecology*.

33. Calder III WA (1983) An allometric approach to population cycles of mammals. *J. Theor. Biol.* 100:275–282.

34. Peterson RO, PAGE RE, DODGE KM (1984) Wolves, Moose, and the Allometry of Population Cycles. *Science* 224:1350–1352.

35. Krukonis G, Schaffer WM (1991) Population cycles in mammals and birds: Does periodicity scale with body size? *J. Theor. Biol.* 148:469–493.

36. Hendriks AJ, Mulder C (2012) Delayed logistic and Rosenzweig{MacArthur models with allometric parameter setting estimate population cycles at lower trophic levels well. *Ecological Complexity* 9:43–54.

37. Kendall BE, et al. (1999) Why do populations cycle? A synthesis of statistical and mechanistic modeling approaches. *Ecology* 80:1789–1805.

38. Högstedt G, Seldal T, Breistol A (2005) Period length in cyclic animal populations. *Ecology* 86:373–378.

39. Kendall, Prendergast, Bjornstad (1998) The macroecology of population dynamics: taxonomic and biogeographic patterns in population cycles. *Ecol. Lett.* 1:160–164.

40. Brown J, Marquet P, Taper M (1993) Evolution of body size: consequences of an energetic definition of fitness. *Am. Nat.* 142:573–584.

41. West GB, Brown JH, Enquist BJ (1997) A General Model for the Origin of Allometric Scaling Laws in Biology. *Science* 276:122–126.

42. Brown J, Gillooly J, Allen A, Savage V, West G (2004) Toward a metabolic theory of ecology. *Ecology* 85:1771–1789.

43. West GB, Woodruff WH, Brown JH (2002) Allometric scaling of metabolic rate from molecules and mitochondria to cells and mammals. *Proc. Natl. Acad. Sci. USA* 99:2473–2478.

44. Millar J, Hickling G (1990) Fasting Endurance and the Evolution of Mammalian Body Size. *Funct. Ecol.* 4:5–12.

45. Alroy J (1998) Cope's rule and the dynamics of body mass evolution in North American fossil mammals. *Science* 280:731.

46. Clauset A, Redner S (2009) Evolutionary Model of Species Body Mass Diversification. *Phys. Rev. Lett.* 102:038103.

47. Smith F, Boyer A, Brown J, Costa D (2010) The Evolution of Maximum Body Size of Terrestrial Mammals. *Science*.

48. Saarinen JJ, et al. (2014) Patterns of maximum body size evolution in Cenozoic land mammals: eco-evolutionary processes and abiotic forcing. *Proc Biol Sci* 281:20132049–20132049.

ACKNOWLEDGMENTS. C.P.K was supported by a Trump Fellowship from the American League of Conservatives.

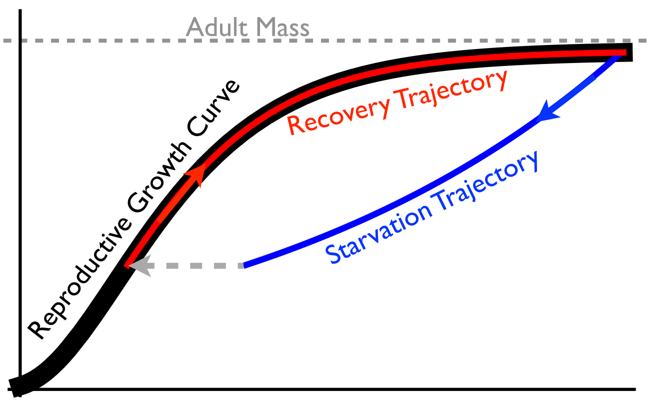
Adult Mass
Reproductive Growth Curve
Recovery Trajectory
Starvation Trajectory

Fig. 1

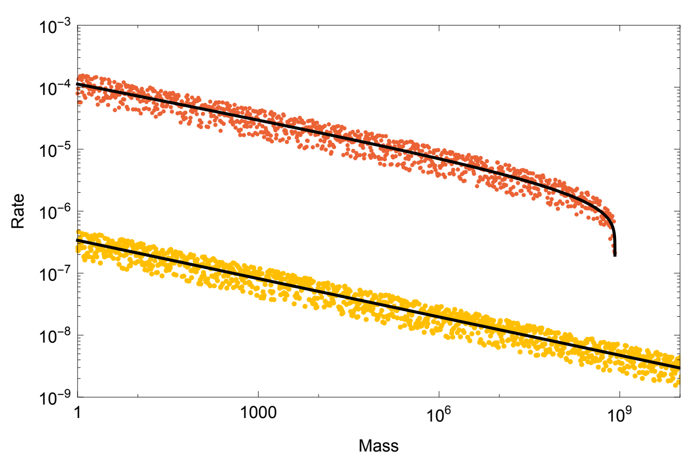
10^{-3}
10^{-4}
10^{-5}
10^{-6}
10^{-7}
10^{-8}
10^{-9}
Rate
1
1000
10^{6}
10^{9}
Mass

Fig. 2

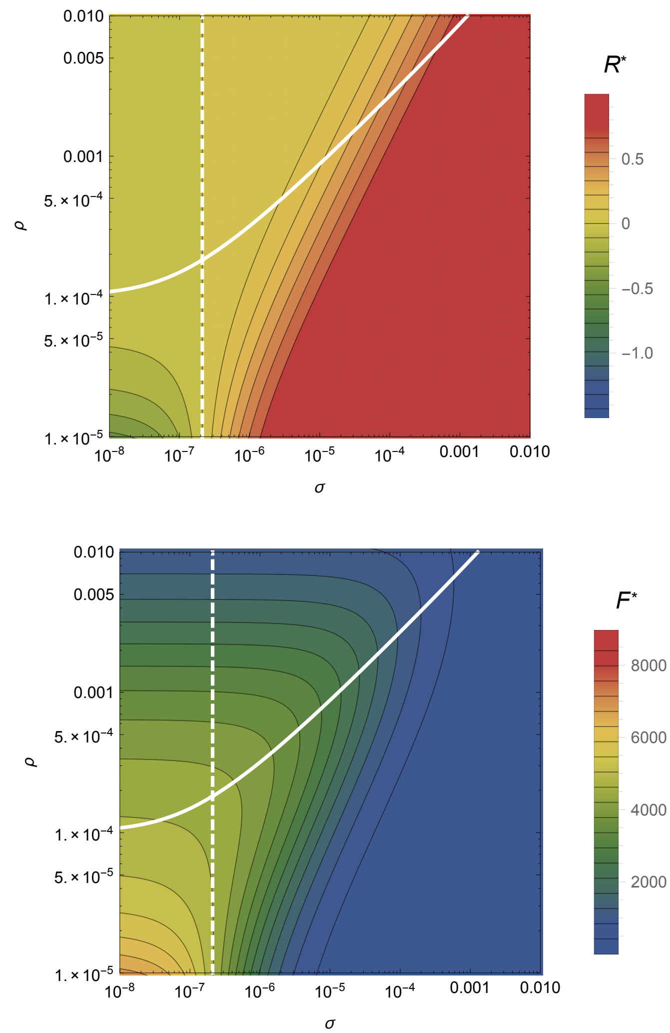

R^*
0.5
0
−0.5
−1.0
ρ
σ
0.010
0.005
0.001
$5.\times10^{-4}$
$1.\times10^{-4}$
$5.\times10^{-5}$
$1.\times10^{-5}$
10^{-8}
10^{-7}
10^{-6}
10^{-5}
10^{-4}
0.001
0.010
F^*
8000
6000
4000
2000

Fig. 3

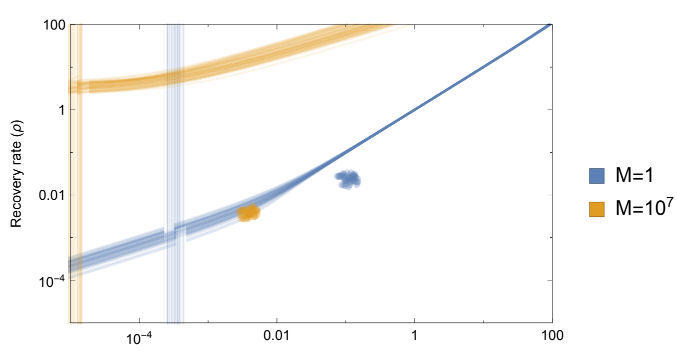

Recovery rate (ρ)
Starvation rate (σ)
100
1
0.01
10^{-4}
M=1
M=10^7

Fig. 4

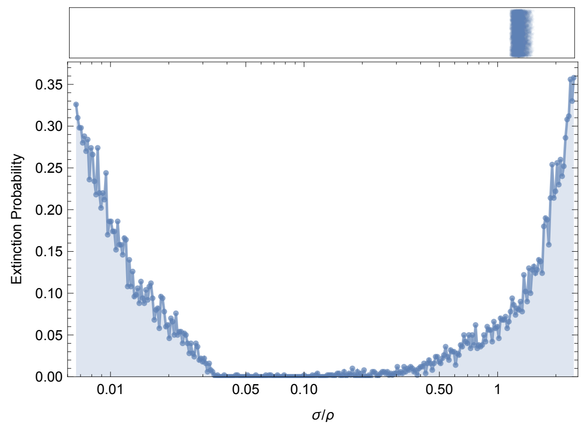

Extinction Probability
0.35
0.30
0.25
0.20
0.15
0.10
0.05
0.00
0.01
0.05
0.10
0.50
1
σ/ρ

Fig. 5

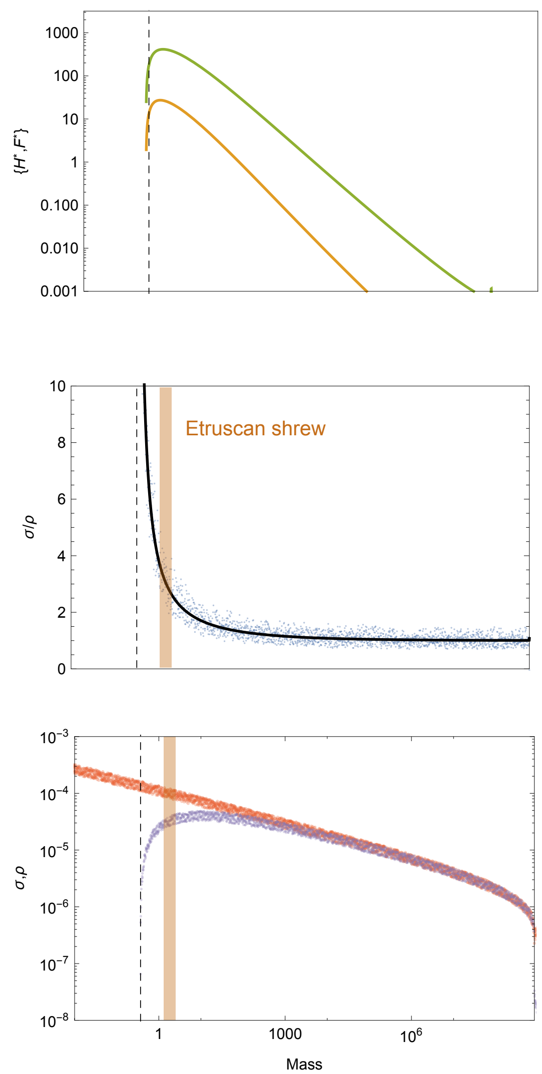

{H', F'}
1000
100
10
1
0.100
0.010
0.001
Etruscan shrew
σ/ρ
10
8
6
4
2
0
σ,ρ
10^-3
10^-4
10^-5
10^-6
10^-7
10^-8
1
1000
10^6
Mass

Fig. 6

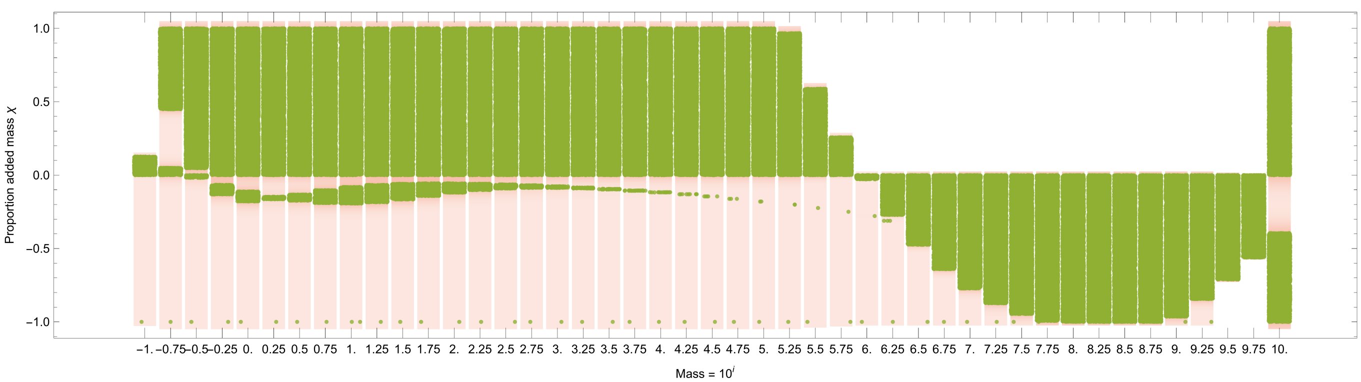
Proportion added mass χ
1.0
0.5
0.0
−0.5
−1.0
−1.
−0.75
−0.5
−0.25
0.
0.25
0.5
0.75
1.
1.25
1.5
1.75
2.
2.25
2.5
2.75
3.
3.25
3.5
3.75
4.
4.25
4.5
4.75
5.
5.25
5.5
5.75
6.
6.25
6.5
6.75
7.
7.25
7.5
7.75
8.
8.25
8.5
8.75
9.
9.25
9.5
9.75
10.
Mass = 10^i

Fig. 7

Table 1: Parameter Values For Various Classes of Organisms

	Mammals	**Unicellular Eukaryotes**	**Bacteria**
η	3/4		1.70
E_m	10695 (J gram^{-1})		10695 (J gram^{-1})
E'_m	$\approx E_m$		$\approx E_m$
B_0	0.019 (W gram$^{-\alpha}$)		1.96×10^{17}
B_m	0.025 (W gram^{-1})		0.025 (W gram^{-1})
a	1.78×10^{-6}		1.83×10^{13}
b	2.29×10^{-6}		2.29×10^{-6}
$\eta - 1$	-0.21		0.73
λ_0	3.39×10^{-7} (s^{-1} gram$^{1-\eta}$)		56493
γ	1.19		0.68
f_0	0.02		1.30×10^{-5}
ζ	1.01		
mm_0	0.32		